COBEM 2021 26th International Congress of Mechanical Engineering
November 22-26, 2021, Virtual Congress, Brazil
ABCM Associação Brasileira de Engenharia e Ciências Mecânicas

COB-2021-1604
A NUMERICAL STUDY ON A TRANSVERSELY ISOTROPIC PERMEABILITY MODEL APPLIED TO SOFT TISSUES

Thayller Weverton Barp
GRANTE - Department of Mechanical Engineering, Federal University of Santa Catarina, Florianópolis, SC, Brazi.
thayller.barp@posgrad.ufsc.br

Bruno Klahr
GRANTE - Department of Mechanical Engineering, Federal University of Santa Catarina, Florianópolis, SC, Brazil.
bruno.klahr@posgrad.ufsc.br

Thiago André Carniel
LaTEM - Laboratory of Process and Technology in Materials, Community University of Chapecó Region, Chapecó, SC, Brazil.
thiago.carniel@unochapeco.edu.br

Eduardo Alberto Fancello
GRANTE - Department of Mechanical Engineering, Federal University of Santa Catarina, Florianópolis, SC, Brazil.
eduardo.fancello@ufsc.br

Abstract. *Fibrous soft biological tissues are mainly composed of water, a cellular matrix and collagen fibers. Due to the poorly vascularization of such tissues, solute transport and cell nutrition are likely to be ruled by diffusive phenomena by means of interstitial fluid flow. In order to investigate mechanisms associated with the fluid flow, biphasic models, have been widely used to investigate the mechanical behavior of soft biological tissues. In some tissues, due to the organization of the collagen fiber network, the interstitial flow may be strongly dependent on the fibers' orientation. Motivated by these observations, this work aims to investigate the influence of fiber direction on the interstitial flow. To this end, a biphasic formulation in finite deformations with the classic Darcy law to represent the fluid flow behavior was employed. To incorporate the influence of the fibrous structure on the fluid flow, a transversely isotropic permeability model is derived. The biphasic governing equations are discretized by the finite element method, using an iterative sequential strategy for solving the coupled problem. To validate the proposed formulation, a numerical confined compression test was performed on a home-made finite element code and compared with the results obtained from a commercial FEM software. The results show that the proposed formulation is capable to represent the fluid flow oriented by fibers.*

Keywords: *Poroelasticity, finite element method, transversely isotropic permeability, soft biological tissues.*

1. INTRODUCTION

Biological tissues are formed primarily by specialized cells and extracellular matrix (ECM). This composition allows us to classify them as composite materials, whose constituents have great adaptability to the physiological environment, especially in relation to the mechanical behavior. The understanding of the correlation between the biomechanical behavior and the mechanisms responsible for adaptation and repair is essential for tissue function (Cowin and Doty, 2007; Ehret *et al.*, 2017).

Besides cells and ECM, soft biological tissues are mainly composed of water (Ehret *et al.*, 2017). However, many soft tissues, *e.g.*, connective tissues, are poorly vascularized. In this case, the main mechanism of nutrients transport consists of diffusive ways. Thus, the incorporation of such phenomena in computational models that aim to investigate the biomechanical behavior of these tissues becomes essential.

In this context, poroelasticity theories, first proposed for geomechanical studies (Terzaghi, 1923; Biot, 1941), emerges as a suitable strategy to investigate the influence of the interstitial flow. The fields associated with mechanical behavior can be investigated in a computational environment, complementing experimental observations. This theory allows approaching the biological tissues as a multiphase and anisotropic material, making it possible to visualize the contribution of the fluid in the mechanical response of the tissue (Gustafsson, 2014).

To investigate these phenomena in a computational context, biphasic models are commonly employed (Mow *et al.*, 1980; Lai *et al.*, 1981; Holmes and Mow, 1990; Suh *et al.*, 1991; Almeida and Spilker, 1997). The resistance to interstitial flow in the structures of these tissues contribute to the morphogenesis of capillaries and lymphatic vessels, indicating the

correlation between the flow and mechanisms of cell mechanotransduction (Danziger and Zeidel, 2015; Thompson *et al.*, 2017). In addition, in some connective fibrous tissues, an anistropic behavior of this fluid flow resistance is observed (Ateshian and Weiss, 2010).

Motivated by these observations, the main goal of this paper is to present preliminary results within the context of the mechanical behavior of soft biological tissues. In order to incorporate diffusion effects, a poroelastic model under finite strain regime is employed. With the particular goal of investigating the anisotropic mechanical characteristics of fluid flow, a fiber oriented permeability model is formulated for the fluid flow. Aiming to verify this model, a numerical example based on a confined compression case was simulated and the results were compared with those obtained using a commercial finite element (FEM) software.

The purpose of this research consist in the development of a numerical approach enabling future investigations involving the characteristics of fibers and their relationship with the anisotropy of the interstitial fluid flow in biological tissues. The research on biphasic behavior of fibrous biological tissues aims to clarify diffusive mechanisms that may lead to cell nutrition, pathological and healing process.

2. POROELASTICITY AT FINITE STRAINS

Poroelasticity models are commonly used to represent the mechanical behavior of porous media, which are usually defined by means of two or more material phases. In the case of biphasic models, there is a fluid phase flowing through a solid porous structure. In this study, the porous medium is considered a homogenized medium, *i.e.*, the phases of the material are assumed to compose a single biphasic continuous medium, where no explicit separation is made between the fluid and solid phases. The basic fundamentals of the biphasic theory presented in this paper are based on the following references: Levenston *et al.* (1998); Armero (1999); Coussy (2003); Cheng (2016); Dormieux *et al.* (2006); Hirabayashi and Iwamoto (2018)

2.1 Theoretical background

The biphasic model describes the mechanics of a mixture between a solid and a fluid phase. Figure 1 represents the spatial and material domains of the mixture, where the spatial configuration is formed by a single continuum. The reference configuration treats each phase as a distinct domain, being Ω^{f}_X e Ω^{s}_X the fluid and solid domains, respectively.

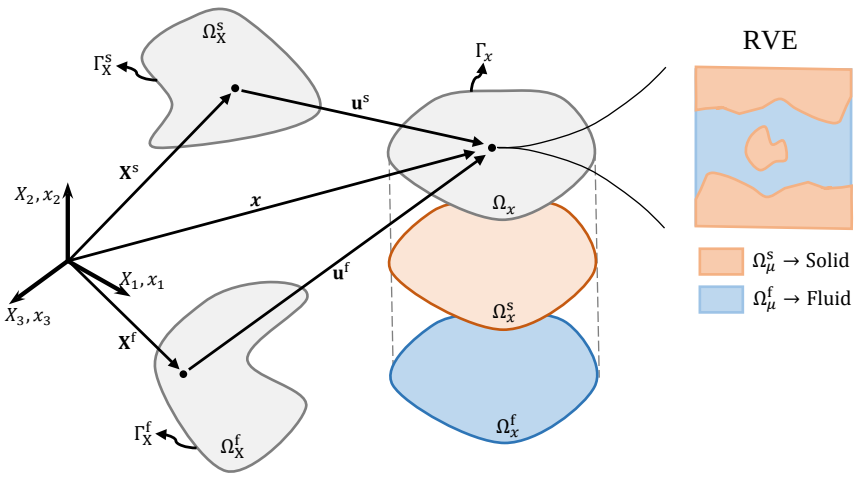

Figure 1. Referential and spatial macroscopic representations of the biphasic domain. Schematic representation of a representative volume element (RVE) of a biphasic material.

It is observed that the position of a spatial point $\mathbf{x}$ can be described by both phases,

$$\mathbf{x} = \mathbf{X}^{\mathrm{s}} + \mathbf{u}^{\mathrm{s}} = \mathbf{X}^{\mathrm{f}} + \mathbf{u}^{\mathrm{f}}, \tag{1}$$

where the notations $(\cdot)^{\mathrm{s}}$ and $(\cdot)^{\mathrm{f}}$ are used to denote the solid and fluid phases, respectively. The vector $\mathbf{X}$ is the position of the point in the reference configuration and $\mathbf{u}$ is the displacement vector. The deformation gradients and volumetric Jacobians of each phase are given by,

$$\mathbf{F}^{\mathrm{s}} = \frac{\partial \mathbf{x}}{\partial \mathbf{X}^{\mathrm{s}}}, \mathbf{F}^{\mathrm{f}} = \frac{\partial \mathbf{x}}{\partial \mathbf{X}^{\mathrm{f}}}, \tag{2}$$

$$J^{\mathrm{s}} = \det\left(\mathbf{F}^{\mathrm{s}}\right), J^{\mathrm{f}} = \det\left(\mathbf{F}^{\mathrm{f}}\right). \tag{3}$$

In the spatial configuration, it is considered that both phases coexist in the same space. Thus, the differential volume elements at the macroscopic scale are the same for both phases, represented by,

$$dv = dv^{\mathrm{s}} = dv^{\mathrm{f}}, \tag{4}$$

which can be rewritten in the reference configuration with the help of the Jacobian, *i.e.*:

$$dv^{\mathrm{s}} = J^{\mathrm{s}} dV^{\mathrm{s}}, dv^{\mathrm{f}} = J^{\mathrm{f}} dV^{\mathrm{f}}. \tag{5}$$

It is commonly considered that both phases in a biphasic material are immiscible, *i.e.*, it is possible to distinguish each phase of the mixture. This assumption makes it possible to present the volumetric ratios of each phase, solid and fluid, separately. Considering the microscopic differential of Fig. 1 on a microscopic scale, and using the notation $\alpha = (\mathrm{s}; \mathrm{f})$ to represent the solid and fluid phases respectively, the volume fractions are expressed by,

$$\phi_x^\alpha = \frac{dv_\mu^\alpha}{dv}, \tag{6}$$

where the notation $(\cdot)_\mu$ represents the microscopic scale of the material. Thus, the intrinsic density of each microconstituent can be calculated by the relation,

$$\rho_\mu^\alpha = \frac{dm^\alpha}{dv_\mu^\alpha}. \tag{7}$$

In addition to these initial definitions, four constitutive hypotheses are used for the proposition of the governing equations. Firstly, the microconstituents are considered incompressible, *i.e.*, it is considered that each microconstituent of the RVE has the null density rate, $\dot{\rho}_\mu^\alpha = 0$. Secondly, the mixture is assumed fully saturated, and with no voids within the domain, *i.e.*: $\phi^{\mathrm{s}} + \phi^{\mathrm{f}} = 1$. Thirdly, it is considered an additive decomposition of the total stress, where the Cauchy stress $\boldsymbol{\sigma}$ can be decomposed additively by $\boldsymbol{\sigma} = \boldsymbol{\sigma}^{\mathrm{s}} + \boldsymbol{\sigma}^{\mathrm{f}}$. At last, it is assumed that the contribution of stress related to the fluid $\boldsymbol{\sigma}^{\mathrm{f}}$ depends exclusively of the pore pressure p^{f}, *i.e.*, $\boldsymbol{\sigma}^{\mathrm{f}} = -p^{\mathrm{f}}\mathbf{I}$, where $\mathbf{I}$ represents the identity tensor (Levenston *et al.*, 1998; Armero, 1999; Hirabayashi and Iwamoto, 2018).

In view of the aforementioned hypotheses, the boundary value problem is defined as,

$$\begin{cases} \mathrm{div}\boldsymbol{\sigma} = 0; & \boldsymbol{\sigma} = \boldsymbol{\sigma}^{\mathrm{s}} - p^{\mathrm{f}}\mathbf{I} \\ \mathrm{div}\left(\mathbf{v}^{\mathrm{s}} + \mathbf{w}\right) = 0; & \mathbf{w} \overset{\mathrm{def}}{=} \phi^{\mathrm{f}}\left(\mathbf{v}^{\mathrm{f}} - \mathbf{v}^{\mathrm{s}}\right). \end{cases} \tag{8}$$

where the vector $\mathbf{w}$ represents the relative velocity, the vector $\mathbf{v}^{\mathrm{s}}$ represents the velocity of the solid and the vector $\mathbf{v}^{\mathrm{f}}$ the velocity of the fluid. Equation (8-1) represents the mechanical balance and the Eq. (8-2) represents the conservation of mass. In addition, the boundary conditions are given by:

$$\begin{cases} \mathbf{u}^{\mathrm{s}} = \bar{\mathbf{u}}^{\mathrm{s}} & \mathrm{em}\ \Gamma_u^{\mathrm{s}} \\ \mathbf{t}^{\mathrm{s}} = \boldsymbol{\sigma}\mathbf{n} = \bar{\mathbf{t}}^{\mathrm{s}} & \mathrm{em}\ \Gamma_t^{\mathrm{s}} \\ p^{\mathrm{f}} = \bar{p}^{\mathrm{f}} & \mathrm{em}\ \Gamma_p^{\mathrm{f}} \\ q^{\mathrm{f}} = \mathbf{w}\cdot\mathbf{n} = \bar{q}^{\mathrm{f}} & \mathrm{em}\ \Gamma_q^{\mathrm{f}}. \end{cases} \tag{9}$$

The vector $\bar{\mathbf{u}}^{\mathrm{s}}$ represents a prescribed displacement in the solid boundary Γ_u^{s}, $\bar{\mathbf{t}}^{\mathrm{s}}$ represent a prescribed traction vector on the solid surface Γ_t^{s}, $\bar{p}^{\mathrm{f}}$ represent a prescribed pressure on the boundary Γ_p^{f} and, finally, $\bar{q}^{\mathrm{f}}$ represent a fluid flux on the boundary Γ_q^{f}.

Aiming to solve the biphasic problem using the finite element approach, the weak form of the problem is required. Using the principle of virtual work, the weak form of the problem (8) is given by,

$$\begin{cases} \delta W^{\mathrm{s}} = \displaystyle\int_{\Omega_{\boldsymbol{x}}} \boldsymbol{\sigma}^{\mathrm{s}} : \delta\mathbf{e}^{\mathrm{s}}\,\mathrm{d}v - \int_{\Omega_{\boldsymbol{x}}} p^{\mathrm{f}}\mathrm{tr}\left(\delta\mathbf{e}^{\mathrm{s}}\right)\,\mathrm{d}v - \int_{\Gamma_{\mathrm{t}}^{\mathrm{s}}} \bar{\mathbf{t}}_{\boldsymbol{x}}^{\mathrm{s}} \cdot \delta\mathbf{u}^{\mathrm{s}}\,\mathrm{d}a = 0, \qquad \forall\,\delta\mathbf{u}^{\mathrm{s}} \in \mathcal{K}^{\mathrm{s}} \\ \\ \delta W^{\mathrm{f}} = \displaystyle\int_{\Omega_{\boldsymbol{x}}} \delta p^{\mathrm{f}}\mathrm{div}_{\boldsymbol{x}}\left(\mathbf{v}^{\mathrm{s}}\right)\,\mathrm{d}v - \int_{\Omega_{\boldsymbol{x}}} \boldsymbol{\nabla}_{\boldsymbol{x}}\delta p^{\mathrm{f}} \cdot \mathbf{w}\,\mathrm{d}v + \int_{\Gamma_{\mathrm{q}}^{\mathrm{f}}} \delta p^{\mathrm{f}}\bar{q}^{\mathrm{f}}\,\mathrm{d}a = 0, \qquad \forall\,\delta p^{\mathrm{f}} \in \mathcal{K}^{\mathrm{f}} \end{cases} \tag{10}$$

where $\delta \mathbf{e}^{\mathrm{s}}$ represents the variation of the Almansi strain tensor. Moreover, $\mathcal{K}^{\mathrm{s}}$ and $\mathcal{K}^{\mathrm{f}}$ represent the admissible spaces for the variations $\delta \mathbf{u}^{\mathrm{s}}$ and δp^{f}, respectively.

2.2 Transversely isotropic permeability model

The mechanics of the interstitial fluid was described in the mid-19th century by Henry Darcy, which culminated in the development of the Darcy's Law, given by,

$$\mathbf{w} = -\mathbf{k}^{\mathrm{f}} \nabla_x p^{\mathrm{f}}, \tag{11}$$

where $\nabla_x p^{\mathrm{f}}$ represents the pore pressure spatial gradient and $\mathbf{k}^{\mathrm{f}}$ represents the permeability tensor.

One of the main components controlling diffusive properties in connective tissues is the anisotropic network of collagen fibers. Some studies show that water diffusion is restricted by the presence of the collagen fiber bundles, especially in the fiber normal direction (Pierce *et al.*, 2013; de Visser *et al.*, 2008). In order to consider this anisotropic flow characteristics, a transversely isotropic flow model guided by the axial directions of the fibers is derived.

Considering a local coordinate system (1,2,3) with the axis 1 coincident with the local axial direction of the fiber, the local permeability tensor $\mathbf{k}^{\mathrm{L}}$ is given by,

$$\mathbf{k}^{\mathrm{L}} = \begin{bmatrix} k^a & 0 & 0 \\ 0 & k^t & 0 \\ 0 & 0 & k^t \end{bmatrix} \tag{12}$$

where k^a is the axial permeability parameter (in the local direction of the fibers) and k^t is the transverse permeability parameter. However, it is necessary to represent this tensor in a global coordinate system. The relationship between local and global coordinate systems is established through a rotation matrix $\mathbf{Q}$ (Holzapfel, 2000). Therefore, the global permeability tensor is related to the local one by means of the relation,

$$\mathbf{k}^{\mathrm{G}} = \mathbf{Q}^{\mathrm{T}} \mathbf{k}^{\mathrm{L}} \mathbf{Q}. \tag{13}$$

In this study, the variables $(\cdot)^{\mathrm{G}}$ are referred to the global coordinate system and $(\cdot)^{\mathrm{L}}$ to the local one. Taking into account the components,

$$\mathbf{Q} = \begin{bmatrix} Q_{11} & Q_{12} & Q_{13} \\ Q_{21} & Q_{22} & Q_{23} \\ Q_{31} & Q_{32} & Q_{33} \end{bmatrix}. \tag{14}$$

The vectors that comprise the columns of $\mathbf{Q}$ are orthonormal, resulting in the following restrictions,

$$\begin{cases} Q_{11}Q_{12} + Q_{21}Q_{22} + Q_{31}Q_{32} = 0 \\ Q_{11}Q_{13} + Q_{21}Q_{23} + Q_{31}Q_{33} = 0 \\ Q_{12}Q_{13} + Q_{22}Q_{23} + Q_{32}Q_{33} = 0 \\ Q_{11}^2 + Q_{21}^2 + Q_{31}^2 = 1 \\ Q_{12}^2 + Q_{22}^2 + Q_{32}^2 = 1 \\ Q_{13}^2 + Q_{23}^2 + Q_{33}^2 = 1. \end{cases} \tag{15}$$

In view of Eqs. (13) and (15), and considering the symmetry of the $\mathbf{k}^{\mathrm{G}}$ tensor, the global permeability tensor can be written as,

$$\mathbf{k}^{\mathrm{G}} = \begin{bmatrix} k^a Q_{11}^2 + k^t \left(1 - Q_{11}^2\right) & k^a Q_{11}Q_{12} + k^t \left(-Q_{11}Q_{12}\right) & k^a Q_{11}Q_{13} + k^t \left(-Q_{11}Q_{13}\right) \\ k^a Q_{11}Q_{12} + k^t \left(-Q_{11}Q_{12}\right) & k^a Q_{12}^2 + k^t \left(1 - Q_{12}^2\right) & k^a Q_{12}Q_{13} + k^t \left(-Q_{12}Q_{13}\right) \\ k^a Q_{11}Q_{13} + k^t \left(-Q_{11}Q_{13}\right) & k^a Q_{12}Q_{13} + k^t \left(-Q_{12}Q_{13}\right) & k^a Q_{13}^2 + k^t \left(1 - Q_{13}^2\right) \end{bmatrix}. \tag{16}$$

Furthermore, defining the vector,

$$\mathbf{m} = \begin{bmatrix} m_1 & m_2 & m_3 \end{bmatrix}^{\mathrm{T}}, \tag{17}$$

as the fiber direction, which is coincident with direction 1 of the local coordinate system, one can define the components of the first row of $\mathbf{Q}$ via the direction cosines,

$$Q_{11} = \frac{m_1}{|\mathbf{m}|} \; ; \; Q_{12} = \frac{m_2}{|\mathbf{m}|} \; ; \; Q_{13} = \frac{m_3}{|\mathbf{m}|}. \tag{18}$$

Finally, the global permeability tensor can be expressed as:

$$\mathbf{k}^{\mathrm{G}} = \begin{bmatrix} \left(\frac{m_1}{|\mathbf{m}|}\right)^2 (k^a - k^t) + k^t & \frac{m_1 m_2}{|\mathbf{m}|^2} (k^a - k^t) & \frac{m_1 m_3}{|\mathbf{m}|^2} (k^a - k^t) \\ \frac{m_1 m_2}{|\mathbf{m}|^2} (k^a - k^t) & \left(\frac{m_2}{|\mathbf{m}|}\right)^2 (k^a - k^t) + k^t & \frac{m_2 m_3}{|\mathbf{m}|^2} (k^a - k^t) \\ \frac{m_1 m_3}{|\mathbf{m}|^2} (k^a - k^t) & \frac{m_2 m_3}{|\mathbf{m}|^2} (k^a - k^t) & \left(\frac{m_3}{|\mathbf{m}|}\right)^2 (k^a - k^t) + k^t \end{bmatrix}. \tag{19}$$

2.3 Solution strategy

The system of nonlinear equations (10) is solved using the finite element method. For this purpose, a mixed element formulation are employed, where the solid displacement $\mathbf{u}$ and the pore pressure p^{f} are the primary variables. In the present formulation, an element composed of quadratic interpolation functions is used to approximate the displacement field and linear interpolation functions for the pressure field (Markert, 2008; Berger *et al.*, 2017). This approach is commonly employed in literature in order to avoid numerical instabilities (spurious oscillations in the pressure field).

Considering the time dependent behavior of the problem, a time integration method is required. In this study, a backward Euler method is employed to approximate the solid velocity field. Such strategy provides an implicit and first-order approximation, commonly used in the solution of biphasic problems (Hirabayashi and Iwamoto, 2018; Berger *et al.*, 2017).

In order to solve the nonlinear coupled system resulting from (10), a proper solution strategy must be established. In this work, an iteratively-coupled scheme is employed. Specifically, a coupling algorithm called "*drained*" is used to solve the coupled problem (Kim *et al.*, 2011). Considering this process, for each time increment, Eq. (10-1) is firstly solved considering the fixed pressure field, obtaining the solution for the displacement field. Afterwards, Eq. (10-2) is then solved for the pressure field, keeping the solid displacement field fixed. In this way, this procedure is repeated until a convergence criterion is reached.

3. NUMERICAL EXAMPLE

In order to verify the present model and its implementation, a three-dimensional numerical analysis was proposed and the obtained results are compared with those retrieved by the commercial finite element software Abaqus.

The numerical example investigated consist of simulating a confined compression test usually employed to assess the biphasic behavior of soft tissues. The proposed geometry and the boundary conditions are shown in Fig. 2, where the angle θ represents the fiber orientation on the x-y plane.

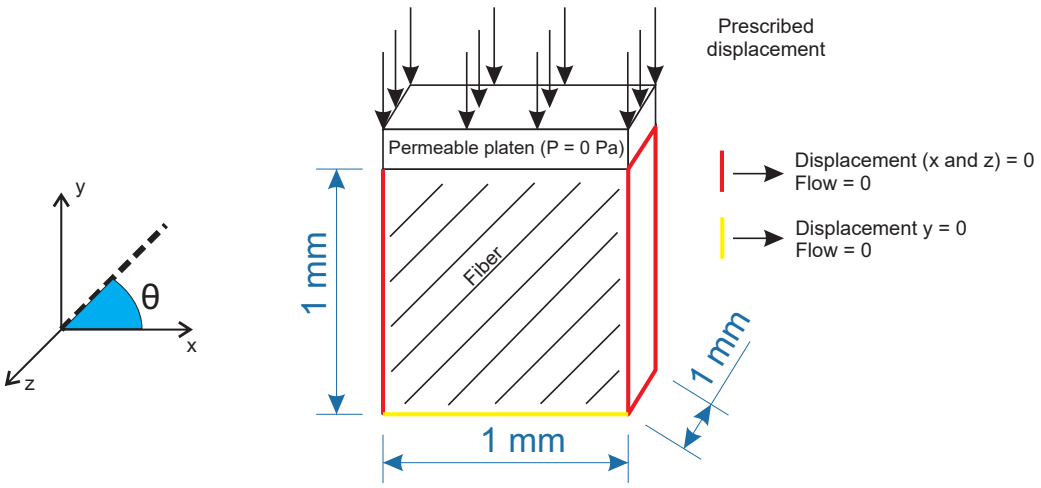

Figure 2. Representation of the geometry and boundary conditions of the confined compression case.

The proposed specimen is a cube of 1 mm edges. In order to apply boundary conditions that entails a confined compression case, displacement constraints are imposed in the y direction at the base of the specimen and in the x and z directions at the lateral boundaries of the specimen. Related to the fluid, zero fluid flow is imposed on all surfaces, except on the upper end of the specimen, where a condition of zero pressure is applied, allowing the fluid flow through this surface.

To simulated a compression experiment, a prescribed displacement of 0.2 mm is applied in y direction on upper surface of the specimen, representing about 20% of nominal elongation. The case intends to simulate a relaxation test. Therefore, it follows two steps. The first one consists of applying the displacement with a constant velocity of 0.0004 mm/s for 500 seconds. The second step consist in a relaxation test, which the prescribed displacement is kept fixed for 1000 seconds.

A Neo-Hookean hiperelastic model is considered for the constitutive behavior of the solid skeleton (Bonet and Wood, 2008), which can be defined by the strain energy function,

$$\psi^s = 2G(\bar{I}_1 - 3) + \frac{K}{2}(J-1)^2. \tag{20}$$

where the parameters $G = 0.343$ MPa and $K = 0.243$ MPa were considered.

For the fluid flow, the Darcy Law with a transversely isotropic permeability of Eq. (19) was used, with the following parameters: $k^a = 0,76\text{x}10^{-2}$ mm^4/Pa.s and $k^t = 0,76\text{x}10^{-3}$ mm^4/Pa.s. These parameters are based on soft tissues permeabilities. It is important to emphasize that, in addition to the local permeability parameters, the transversely isotropic permeability model also requires the direction of fiber orientation. In this study, we used only straight fibers located in the x-y plane with angle $\theta = 45°$, as shown in Fig. 2.

4. RESULTS AND DISCUSSIONS

Figure 3 presents the pore pressure field, obtained from a commercial finite element software and from proposed formulation.

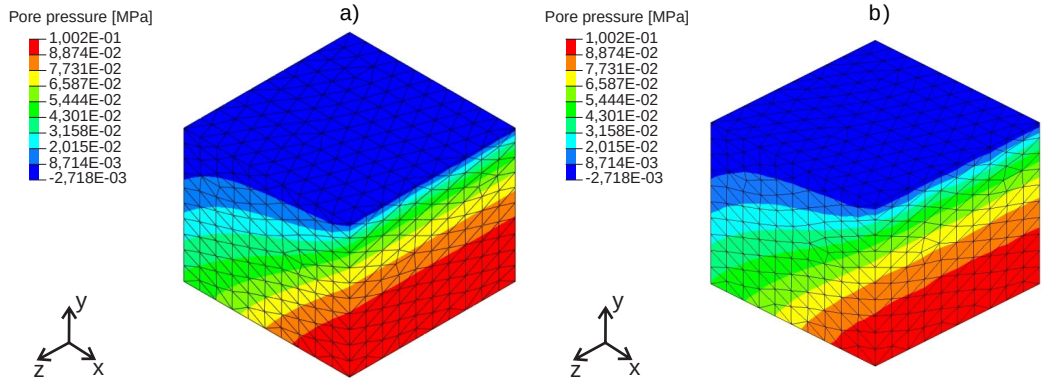

Figure 3. Pore pressure field at $t = 500$ seconds. a) Results obtained from the commercial software Abaqus. b) Results obtained from the implemented model.

It can be seen that similar results were obtained for the pore pressure field in both simulations. The pressure field has a gradual increase in the direction transverse to the fibers, *i.e.*, at $-45°$ from the x-axis in the x-y plane. This observation is supported by Fig. 4, in which the variation of the maximum pore pressure over time is observed. The maximum pore pressure is observed at one of the corners of the specimen base.

Aiming to present the fluid flow direction observed in this example, Fig. 5 presents the relative velocity vectors.

It can be seen that the fibers' alignment constraint the fluid flow to its preferential axial direction, where the largest velocities occur at the right-upper corner of the sample. This clearly reflects the strong anisotropy effect on the fluid flow. The predominant direction observed in the velocity vectors is caused by the higher local axial permeability and due to the imposed boundary conditions of confined compression case.

5. CONCLUSIONS

In this paper a formulation of a poroelasticity model in finite deformations considering a transversely isotropic permeability model was presented. The formulation was implemented in a home-made code, in which a iterative solution method was used in the solution of the coupled problem. In order to verify the proposed formulation and the capability of the permeability model, a confined compression test was simulated on a test case using fibers at 45°.

By comparing the results with a commercial finite element software, similar results were found for both simulations. This illustrate the ability of the permeability model to guide the flow along the direction of fibers within the specimen.

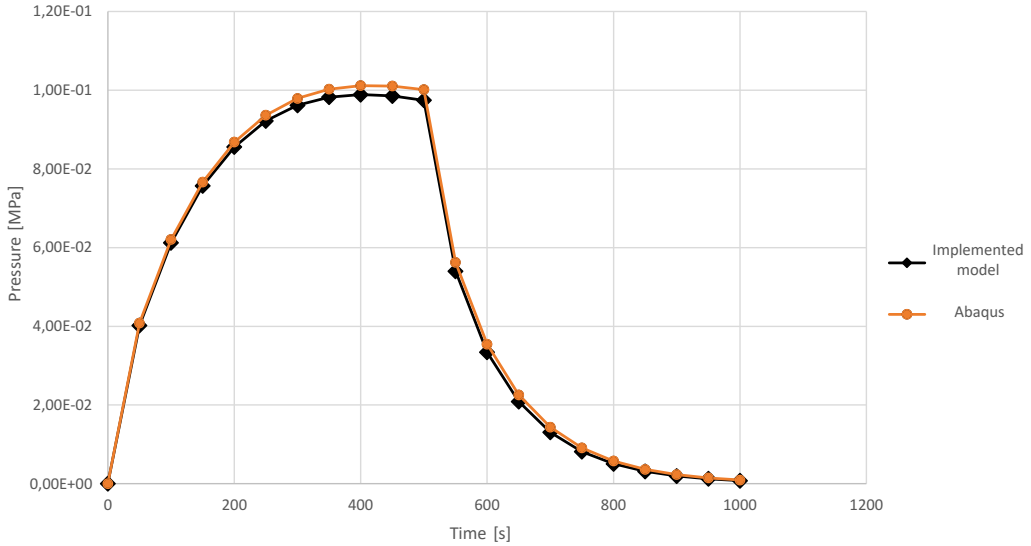

Figure 4. Comparative results of maximum pore pressure versus time.

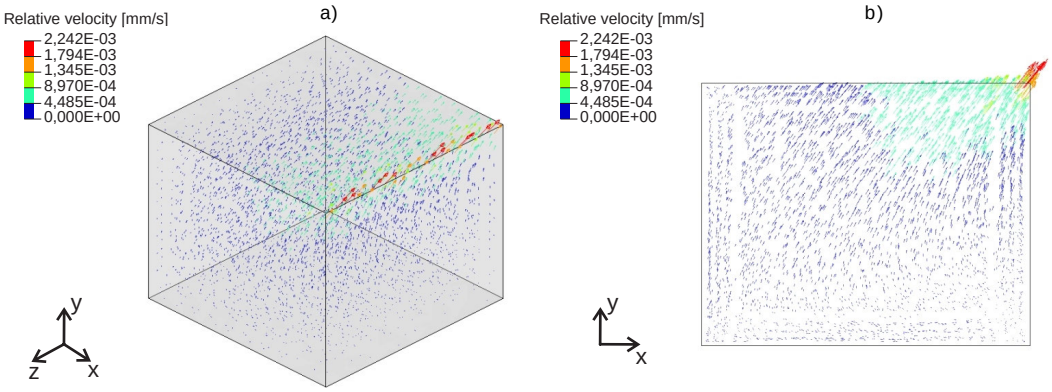

Figure 5. Relative velocity field at $t = 500$ seconds. a) Isometric view. b) X-Y plane view.

At this point it is important to emphasize that this work is part of a research associated with numerical investigations of soft biological tissues. The next steps of this research consist of investigating the anisotropic flow behavior of soft biological tissues by means of phenomenological and multiscale (homogenization) approaches.

6. ACKNOWLEDGEMENTS

The authors would like to thank the financial support provided by the Brazilian funding agencies CAPES - (Coordination for the Improvement of Higher Education Personnel) and CNPq - (National Council for Scientific and Technological Development).

7. REFERENCES

Almeida, E.S. and Spilker, R.L., 1997. "Mixed and Penalty Finite Element Models for the Nonlinear Behavior of Biphasic Soft Tissues in Finite Deformation: Part I - Alternate Formulations". *Computer Methods in Biomechanics and Biomedical Engineering*, Vol. 1, No. 1, pp. 25–46. ISSN 1025-5842. doi:10.1080/01495739708936693. URL `http://www.tandfonline.com/doi/abs/10.1080/01495739708936693`.

Armero, F., 1999. "Formulation and finite element implementation of a multiplicative model of coupled poro-plasticity at finite strains under fully saturated conditions". *Computer Methods in Applied Mechanics and Engineering*, Vol. 171, No. 3-4, pp. 205–241. ISSN 00457825. doi:10.1016/S0045-7825(98)00211-4.

Ateshian, G.A. and Weiss, J.A., 2010. "Anisotropic hydraulic permeability under finite deformation". *Journal of biomechanical engineering*, Vol. 132, No. 11.

Berger, L., Bordas, R., Kay, D. and Tavener, S., 2017. "A stabilized finite element method for finite-strain three-field

poroelasticity". *Computational Mechanics*, Vol. 60, No. 1, pp. 51–68. ISSN 0178-7675. doi:10.1007/s00466-017-1381-8.

Biot, M.A., 1941. "General theory of three-dimensional consolidation". *Journal of Applied Physics*, Vol. 12, No. 2, pp. 155–164. doi:10.1063/1.1712886.

Bonet, J. and Wood, R.D., 2008. *Nonlinear continuum mechanics for finite element analysis*. Cambridge University Press, 2nd edition.

Cheng, A.H.D., 2016. *Poroelasticity*, Vol. 27 of *Theory and Applications of Transport in Porous Media*. Springer International Publishing, Cham. ISBN 978-3-319-25200-1. doi:10.1007/978-3-319-25202-5.

Coussy, O., 2003. *Poromechanics*. John Wiley & Sons, Ltd, Chichester, UK. ISBN 9780470092712. doi:10.1002/0470092718.

Cowin, S.C. and Doty, S.B., 2007. *Tissue mechanics*. Springer Science & Business Media.

Danziger, J. and Zeidel, M.L., 2015. "Osmotic homeostasis". *Clinical Journal of the American Society of Nephrology*, Vol. 10, No. 5, pp. 852–862.

de Visser, S.K., Bowden, J.C., Wentrup-Byrne, E., Rintoul, L., Bostrom, T., Pope, J.M. and Momot, K.I., 2008. "Anisotropy of collagen fibre alignment in bovine cartilage: comparison of polarised light microscopy and spatially resolved diffusion-tensor measurements". *Osteoarthritis and Cartilage*, Vol. 16, No. 6, pp. 689–697.

Dormieux, L., Kondo, D. and Ulm, F.J., 2006. *Microporomechanics*. John Wiley & Sons, Ltd, Chichester, UK. ISBN 9780470032008. doi:10.1002/0470032006.

Ehret, A.E., Bircher, K., Stracuzzi, A., Marina, V., Zündel, M. and Mazza, E., 2017. "Inverse poroelasticity as a fundamental mechanism in biomechanics and mechanobiology". *Nature communications*, Vol. 8, No. 1, pp. 1–10.

Gustafsson, A., 2014. "A fibre-reinforced poroviscoelastic finite element model for the achilles tendon".

Hirabayashi, S. and Iwamoto, M., 2018. "Finite element analysis of biological soft tissue surrounded by a deformable membrane that controls transmembrane flow". *Theoretical Biology and Medical Modelling*, Vol. 15, No. 1, p. 21. ISSN 1742-4682. doi:10.1186/s12976-018-0094-9.

Holmes, M. and Mow, V.C., 1990. "The nonlinear characteristics of soft gels and hydrated connective tissues in ultrafiltration". *Journal of biomechanics*, Vol. 23, No. 11, pp. 1145–1156.

Holzapfel, G., 2000. *Nonlinear solid mechanics: a continuum approach for engineering*. John Wiley & Sons, Chichester.

Kim, J., Tchelepi, H. and Juanes, R., 2011. "Stability and convergence of sequential methods for coupled flow and geomechanics: Drained and undrained splits". *Computer Methods in Applied Mechanics and Engineering*, Vol. 200, No. 23-24, pp. 2094–2116.

Lai, W.M., Mow, V.C. and Roth, V., 1981. "Effects of nonlinear strain-dependent permeability and rate of compression on the stress behavior of articular cartilage". *Journal of Biomechanical Engineering*, Vol. 103, No. 2, pp. 61–66. ISSN 15288951. doi:10.1115/1.3138261.

Levenston, M., Frank, E. and Grodzinsky, A., 1998. "Variationally derived 3-field finite element formulations for quasistatic poroelastic analysis of hydrated biological tissues". *Computer Methods in Applied Mechanics and Engineering*, Vol. 156, No. 1-4, pp. 231–246. ISSN 00457825. doi:10.1016/S0045-7825(97)00208-9.

Markert, B., 2008. "A biphasic continuum approach for viscoelastic high-porosity foams: Comprehensive theory, numerics, and application". *Archives of Computational Methods in Engineering*, Vol. 15, No. 4, pp. 371–446. doi:10.1007/s11831-008-9023-0.

Mow, V.C., Kuei, S., Lai, W.M. and Armstrong, C.G., 1980. "Biphasic creep and stress relaxation of articular cartilage in compression: theory and experiments". *Journal of biomechanical engineering*, Vol. 102, No. 1, pp. 73–84.

Pierce, D.M., Ricken, T. and Holzapfel, G.A., 2013. "A hyperelastic biphasic fibre-reinforced model of articular cartilage considering distributed collagen fibre orientations: continuum basis, computational aspects and applications". *Computer methods in biomechanics and biomedical engineering*, Vol. 16, No. 12, pp. 1344–1361.

Suh, J.K., Spilker, R.L. and Holmes, M.H., 1991. "A penalty finite element analysis for nonlinear mechanics of biphasic hydrated soft tissue under large deformation". *International Journal for Numerical Methods in Engineering*, Vol. 32, No. 7, pp. 1411–1439. ISSN 10970207. doi:10.1002/nme.1620320704.

Terzaghi, K., 1923. "Die Berechnung der Durchlässigkeitszifferdes tones aus dem verlauf der hydrodynamischen spanungserscheinnungen". *Akademie der Wissenschaften in Wien*, pp. 125–138.

Thompson, M.S., Bajuri, M.N., Khayyeri, H. and Isaksson, H., 2017. "Mechanobiological modelling of tendons: Review and future opportunities". *Proceedings of the Institution of Mechanical Engineers, Part H: Journal of Engineering in Medicine*, Vol. 231, No. 5, pp. 369–377.

8. RESPONSIBILITY NOTICE

The authors are solely responsible for the printed material included in this paper.